IEEE Access
Multidisciplinary | Rapid Review | Open Access Journal

Received June 30, 2020, accepted July 10, 2020, date of publication July 27, 2020, date of current version August 11, 2020.

Digital Object Identifier 10.1109/ACCESS.2020.3012132

Predicting Scattering From Complex Nano-Structures via Deep Learning

YONGZHONG LI[1], YINPENG WANG[1], SHUTONG QI[1], QIANG REN[1], (Member, IEEE), LEI KANG[2], SAWYER D. CAMPBELL[2], (Member, IEEE), PINGJUAN L. WERNER[2], (Senior Member, IEEE), AND DOUGLAS H. WERNER[2], (Fellow, IEEE)

[1]School of Electronics and Information Engineering, Beihang University, Beijing 100191, China
[2]Department of Electrical Engineering, The Pennsylvania State University, University Park, PA 16802, USA

Corresponding author: Qiang Ren (qiangren@buaa.edu.cn)

This work was supported in part by the National Natural Science Foundation of China under Grant 61801009, and in part by the Domain Foundation of Equipment Advance Research of the 13th Five-year Plan under Grant 61402090603 and Grant 61402080205.

ABSTRACT Existing numerical electromagnetic (EM) solvers are usually computationally expensive, time consuming, and memory demanding. Recent advances in deep learning (DL) techniques have demonstrated superior efficiency and provide an alternative pathway for speeding up simulations by serving as effective computational tools. In this paper, we propose a DL framework for real-time predictions of the scattering from an isolated nano-structure in the near-field regime. We find that, to achieve precise approximation of the optical response obtained from numerical simulations, the proposed DL framework only requires a small training data set. The fully trained framework can be three orders of magnitude faster than a conventional EM solver based on the finite difference frequency domain method (FDFD). Furthermore, the proposed DL framework has demonstrated robustness to changes in design variables which govern the nano-structure geometry and material selection as well as properties of the incident wave, shedding light on universal scattering predictions at the nano scale via deep learning techniques. This framework increases the viability of the design and analysis of complex nanostructures, offering great potential for applications pertaining to complex light-matter interaction between electromagnetic fields and nanomaterials.

INDEX TERMS Deep learning, nanostructure, nano-optics simulation, scattering analysis, computational electromagetics.

I. INTRODUCTION

Scattering results from the interaction between light and an object or set of objects (e.g., nanoparticles). Accurate predictions of an isolated object's scattered field distribution can be generated using numerical simulations for a given excitation field and is of great importance to a variety of areas related to nanophotonics, including linear and nonlinear responses of nano-particles [1] and nano-antennas [2], [3], metasurfaces [4], [5], biophotonics [6], [7], etc. The total field (the superposition of the incident and scattered fields) of a geometrically-simple scatterer (such as a sphere or cuboid) can be solved either analytically or in a semi-analytical manner, which enables their scattering behaviors to be calculated in an extremely rapid fashion. However, complex scatterers whose shapes may be described by multiple geometrical parameters generally require sophisticated numerical tools which solve complex matrix systems discretized from differential or integral forms of Maxwell's equations. Maxwell's solvers based on finite element methods [8], the method of moments [9], and finite difference methods [10], discontinuous garlekin method [11]–[13] have been developed. Unfortunately, compared to analytical methods, simulations using these tools are generally extremely time consuming and computationally expensive [14]. Nevertheless, fast simulation of optical responses at the nano scale is highly desired in scenarios that require real-time application such as biosensing [15], [16] and iterative inverse designs of complex optical devices [17], [18], analysis of optical chirality [19]. As a result, creating a surrogate EM solver that is capable of real-time calculations for problems involving geometrical, material, and excitation variables is a challenging task.

The associate editor coordinating the review of this manuscript and approving it for publication was Qi Zhou.

Thanks to emerging Deep Learning (DL) techniques [20] such as convolutional neural networks (CNNs), recurrent neural networks (RNNs), and generative adversarial networks (GANs), the field of computational physics has witnessed spectacular advances in physics-learned surrogate modelling [21]. Given large quantities of labeled data and sufficient computing resources (i.e., graphics processing units), DL techniques are able to identify the hidden rules that govern the 'action-reaction' behavior of a system through a certain learning process. It is worth noting that these techniques usually involve the construction of a task-oriented neural network architecture, pre-processing of large-scale training and testing datasets, an end-to-end training and thorough testing. For example, Tompson *et al.* have implemented efficient simulations of Naiver-Stokes equations for optical flow estimation with the assistance of a CNN-based method [22], which exhibited superior performance in terms of accuracy and acceleration rate compared to a traditional solver. Furthermore, CNNs have been introduced for steady flow estimation that is two to four orders of magnitude faster than CPU-based computational fluid dynamics solvers [23]. Moreover, Peurifoy *et al.* [24] have proposed an artificial neural network (ANN) method to estimate light scattering by multiple nanoparticles and have demonstrated an analytical-method based inverse-design by using gradients obtained from backpropagation of the ANN. Besides, Li *et al.* have brought up a DL method to solve Poisson's equation in two-dimensional (2D) [25] and 3D [26] domains for scatterers of basic shapes. This method achieved a noticeable speedup of two orders of magnitude while maintaining a corresponding average relative error as low as 1% for the 2D scenario and 3% for 3D. In addition, two novel DL strategies based on CNNs and RNNs have been proposed to solve the finite difference time domain (FDTD) problem [27]. Recently, a CNN-based model has been developed to predict the solution of Maxwell's equations for low-frequency EM devices [28], including simple coils, transformers, and permanent magnet motors. Towards this end, a data-driven approach was conducted in a supervised manner to learn the distribution of the magnetic field in the vicinity of the components. Very recently, some researchers proposed a DL-based model to predict the absorption response for different plasmonic structures, where a combination of CNN and RNN was applied to conduct the mapping from plasmonic structure to the absorption curve output [29]. In addition to the forward optical analysis, rapid progress has been achieved on the inverse design problems for EM nanostructures during recent year. DL-based techniques along with dimensionality reduction methods greatly facilitate the revealing of underlying phyiscs of light matter interactions in nanophotonics device [30], thus, contributing both the knowledge discovery [31] and device optimization process of EM nanostructures [32].

These emerging DL techniques overcome the drawbacks of previous machine learning methods in which the structural characters of optimized objects are transformed into feature vectors that fail to deliver geometric properties along with the boundary conditions. Therefore, the trained model from machine learning is limited in interpretability and adaptability. However, an inherent problem of employing DL methods is that the proposed surrogate EM solver might fail to provide accurate predictions when the inputs are significantly different from the training samples. If this occurs, the surrogate model's applicability to diverse nanostructure scattering scenarios will be severely limited. Nonetheless, the aforementioned studies related to using deep learning methods to conduct forward near-field electromagnetics analysis often fail to address this problem for three reasons. Firstly, the reported methods are applied to produce surrogate models for scatterers with low complexity or for small-scale applications. Secondly, most of the current DL-based methods are limited to preditions when a set of conditions vary [33], i.e. for different structural models or materials for scatterers, and also for dissimilar illumination configurations, which may degrade the applicability for universial scattering predictions. Thirdly, most existing approaches depend on intelligently selected datasets, which may preclude their generalization to other problems and cast doubt on the realiability of validation for the proposed method.

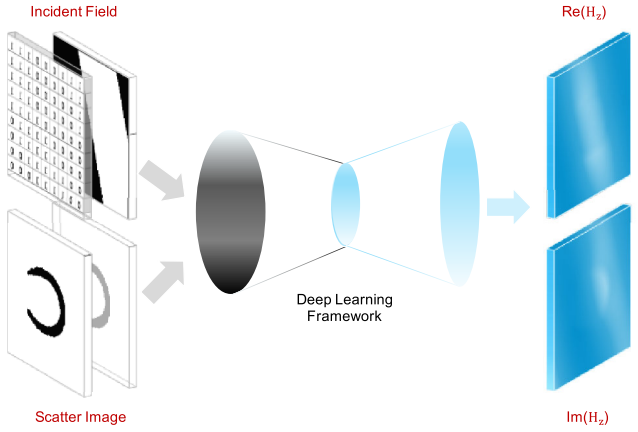

FIGURE 1. Schematic of the deep learning framework which learns to predict the EM fields from the nano scatters.

Here, we develop a DL framework to approximate the simulation of electromagnetic wave scattering from nano-structures (see Figure 1) comprising a range of geometric shapes, orientations, and material values (permittivity, see Table 1) for a number of different illuminations. Our goal is to utilize the DL framework to accurately predict the scattered fields from a complex scatter without directly solving Maxwell's equations. This is accomplished by training the system with samples generated from a series of FDFD simulations. Towards this end, a multilayer CNN-based DL framework inspired by the U-network [34] architecture is proposed. Technically, this framework is trained by 2D image data that is obtained from rigorous scattering calculations. Firstly, 2D datasets, including both the image pairs and ground truth of EM field, are generated by employing an efficient FDFD method. These datasets are then further split into

TABLE 1. Optical properties of selected metals.

Metal	n	k	ε_r
Cu	1.04	0.82	0.41+1.71i
Ag	1.46	0.56	1.82+1.64i
Au	1.37	0.80	1.24+2.19i
Rh	1.17	0.69	0.89+1.61i
Pt	1.46	1.15	0.81+3.36i
Pd	1.14	0.65	0.88+1.48i
Hg	1.06	0.57	0.81+1.20i
Ir	1.45	1.01	1.08+2.93i

two independent subsets which are dedicated to train and test the DL framework. Proof-of-concept demonstrations show that the proposed method can achieve three orders of magnitude computational acceleration without losing accuracy. Furthermore, besides of the numerical acceleration and the refinement of error rate, the DL-based surrogate EM solver is valued for its robust generalizability to accurately predict responses from random inputs; a scenario not covered by the training datasets. To further validate the generalizability of the network, an open-source dataset is evaluated and the results show excellent agreement with those obtained from COMSOL Multiphysics [35] simulations. It should be noted that our framework only requires a single on-line training and can be used to map random inputs with their corresponding EM fields using an off-line prediction.

This paper is organized as follows. In Section II, we introduce the generation of 2D datasets and the proposed CNN framework architecture. In Section III, the proposed framework is verified by numerical results and detailed summaries of the accuracy and speed-up of the network are provided to support its verification. Finally, conclusions are provided in Section IV.

II. METHODOLOGY AND FORMULATION

Within the proposed framework, 2D domains are used to train and evaluate the nanostructure scatterers. The first step in realizing the trained DL model is to generate a sufficient dataset consisting of both training and testing samples of various 2D nanostructures. In this case, efficient traditional EM solvers are of vital importance to generate a large quantity of data. Herein, we combine an FDFD solver with an arbitrary scatterer shape generator in MATLAB to produce the requisite datasets.

A. FINITE DIFFERENCE FREQUENCY DOMAIN (FDFD)

In the frequency domain, Maxwell's equations can be written as follows:

$$\nabla \times \boldsymbol{E} = -i\omega\mu\boldsymbol{H} \tag{1}$$
$$\nabla \times \boldsymbol{H} = i\omega\dot{\varepsilon}\boldsymbol{E} + \boldsymbol{J} \tag{2}$$

where $\boldsymbol{E}$, $\boldsymbol{H}$ represent the electric and magnetic fields, respectively, while $\boldsymbol{J}$ denotes the electric current source, $\dot{\varepsilon}$ is the complex permittivity, and μ is the permeability. The complex permittivity can be written as,

$$\dot{\varepsilon} = \varepsilon_1 + i\varepsilon_2 \tag{3}$$

Moreover, we define $\dot{N}$ as the complex index of refraction,

$$\dot{N} = n + ik \tag{4}$$

where n is the refractive index, and k is the extinction coefficient. Since $\dot{\varepsilon} = \dot{N}^2$, one can rewrite $\dot{\varepsilon}$ as:

$$\varepsilon_1 = n^2 - k^2 \tag{5}$$
$$\varepsilon_2 = 2nk \tag{6}$$
$$\dot{\varepsilon} = \left(n^2 - k^2\right) + i\,(2nk) \tag{7}$$

Note that the wavelength of light is related to the photon energy by,

$$\lambda = \frac{1.2398}{E} \tag{8}$$

where E is photon energy, which is expressed in electron volts (eV). The CRC handbook [36] can be used as a reference for the optical properties of selected dispersive media by tabulating the relationship between photon energy and n, k. Herein, optical properties of several lossy metallic media at a free space wavelength of $\lambda = 123.98nm$ are listed in table 1, all the listed materials are used for scattering analysis.

In a cartesian coordinates system, scalar form of maxwell's equations can be expressed as follows:

$$\frac{\partial E_z}{\partial y} - \frac{\partial E_y}{\partial z} = -i\omega\mu H_x \quad \frac{\partial H_z}{\partial y} - \frac{\partial H_y}{\partial z} = i\omega\dot{\varepsilon}E_x + J_x \tag{9}$$
$$\frac{\partial E_z}{\partial x} - \frac{\partial E_x}{\partial z} = -i\omega\mu H_y \quad \frac{\partial H_z}{\partial x} - \frac{\partial H_x}{\partial z} = i\omega\dot{\varepsilon}E_y + J_y \tag{10}$$
$$\frac{\partial E_x}{\partial y} - \frac{\partial E_y}{\partial x} = -i\omega\mu H_z \quad \frac{\partial H_x}{\partial y} - \frac{\partial H_y}{\partial x} = i\omega\mu E_z + J_z \tag{11}$$

We can approximate the derivatives by a central difference scheme in a Cartesian coordinate system and transform them into a set of scalar differential equations.

$$\frac{E_z^{i,j+1,k} - E_z^{i,j,k}}{\Delta y} - \frac{E_y^{i,j,k+1} - E_y^{i,j,k}}{\Delta z} = -i\omega\mu_x^{i,j,k} H_x^{i,j,k} \tag{12}$$
$$\frac{E_z^{i+1,j,k} - E_z^{i,j,k}}{\Delta x} - \frac{E_x^{i,j,k+1} - E_x^{i,j,k}}{\Delta z} = -i\omega\mu_y^{i,j,k} H_y^{i,j,k} \tag{13}$$
$$\frac{E_x^{i,j+1,k} - E_x^{i,j,k}}{\Delta y} - \frac{E_y^{i+1,j,k} - E_y^{i,j,k}}{\Delta x} = -i\omega\mu_z^{i,j,k} H_z^{i,j,k} \tag{14}$$

where i, j, k represent the locations for the subdomain in the mesh grid. The above differential equations can be further cast into matrix form as follows:

$$C_e\boldsymbol{e} = -i\omega D_\mu \boldsymbol{h} \tag{15}$$
$$C_h\boldsymbol{h} = i\omega D_{\dot{\varepsilon}}\boldsymbol{e} + \boldsymbol{J} \tag{16}$$

where C_e and C_h are matrices for the curl operators on the electric and magnetic fields, while D_μ and $D_{\dot{\varepsilon}}$ are diagonal matrices for the permeability and complex permittivity,

respectively. The system of equations can be simplified by eliminating $\boldsymbol{e}$, and reduces to the following expression:

$$\left(\boldsymbol{C}_h - \omega^2 \boldsymbol{D}_{\hat{\varepsilon}} \boldsymbol{C}_e^{-1} \boldsymbol{D}_\mu\right) \boldsymbol{h} = \boldsymbol{j} \tag{17}$$

Then we apply a direct solver or iterative solver [37], [38] to obtain the EM field solutions for the unknown $\boldsymbol{h}$. It is worth noting that the DL framework is employed to approximate the matrix system $\left(\boldsymbol{C}_h - \omega^2 \boldsymbol{D}_{\hat{\varepsilon}} \boldsymbol{C}_e^{-1} \boldsymbol{D}_\mu\right)^{-1}$ for every input.

B. 2D DATASET GENERATION

Deep neural networks require ground truth simulations to train and optimize their internal parameters to learn how to perform a chosen task. The 2D scatterers of interest here can have complex shapes (such as circles, ovals, triangles, quadrilaterals, pentagons, and their combinations) as well as a wide range of material properties. Therefore, each dataset may contain samples with distinct scatterer characteristics including size, shape, location and permittivity. Continuous representations of the 2D scatterer geometries are then projected onto a 128 × 128 Cartesian grid in order to calculate their corresponding magnetic fields using the FDFD solver. The field data is then used as training labels in the DL framework. Vacuum was chosen as the background medium, while the scatterer is randomly selected from the set of eight materials listed in Tab. 1. The total-field scattered-field source is y-polarized along any directions in the x-y plane and at the wavelength of 123.98 nm under which we treated the target materials with nano-structure as lossy dielectrics, not metal. All these different illumination and material settings can be find in almost all the figures related to demonstrations of numerical results. In order to prevent reflection from the ends of the truncated simulation domain, the boundary conditions are set as perfectly matched layers (PML). The overall dataset contains 36,000 sets of data, with 6,000 arbitrary samples for each category of different complex shapes, in which 90 percent of total samples serve as the training set and the rest are used to test the predicted results after training. It is worth mentioning that all sets of data is obtained from FDFD strictly solving process under certain illumination settings. Furthermore, an open source dataset [39] is adopted to further validate the generalizability of the proposed DL framework. This dataset contains over 1,000 random geometric shapes that resemble real-world objects. The same simulation procedure used to produce the EM fields for the training data, including randomly assigning optical properties to different geometries and FDFD solving process under certain illumination settings, is also used to calculate the fields for the open source data set. It should be noted that the open source dataset is not used on the DL framework training, but rather only to test the accuracy of the network after training.

Additionally, the aforementioned calculated results are randomly selected to compare with those obtained from COMSOL Multiphysics to verify the accuracy of the FDFD solver. A summary of one of these comparisons is presented in Fig. 2. The real and imaginary parts of the scatterer's

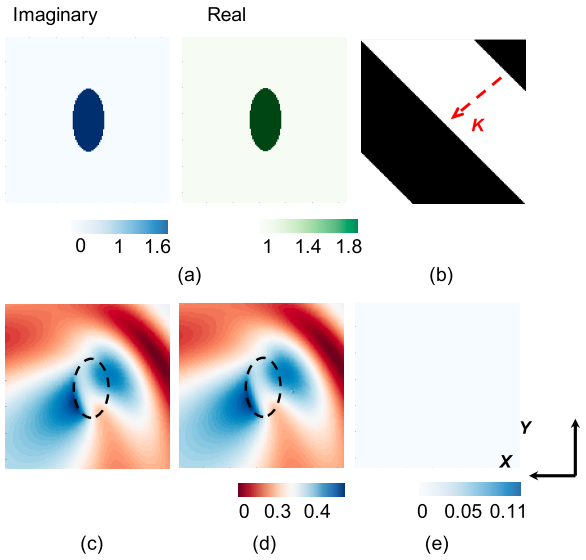

FIGURE 2. Comparison between COMSOL and FDFD. (a) Geometric shape and complex permittivity of the scatterer, (b) Propagation direction of the incident wave, (c) Distribution of $|H_z|$ solved by the FDFD technique, (d) Distribution of $|H_z|$ solved by COMSOL, (e) Error distribution of $|H_z|$ between the FDFD solver and COMSOL.

permittivity are shown in Figs. 2(a). The scatterer (ellipse-shaped) is located at the center of the domain with a semi-major axis of 24 nm and a semi-minor axis of 12 nm. The incident wave is shown in (b) and is a TE plane wave, propagating along the x-axis and polarized along the y-axis. The simulation results obtained from the FDFD solver and COMSOL Multiphysics are shown in Figs. 2(c) and 2(d), respectively. The error distribution which is defined by the absolute difference between the two methods is shown in Fig. 2(e). From this comparison, one can see that the FDFD results agree well with those generated by COMSOL Multiphysics. Therefore, the proposed FDFD solver can be confidently used to generate abundant training data for the following study as a result of its high accuracy and high computational efficiency compared with COMSOL Multiphysics.

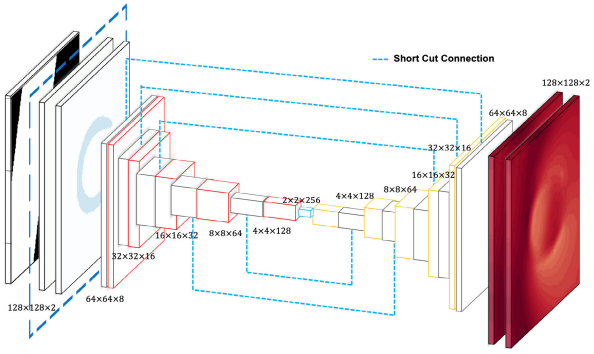

FIGURE 3. Architecture of the deep learning framework and input-output scheme.

C. DEEP LEARNING FRAMEWORK

The proposed deep learning framework and its hyperparameters are shown in Fig. 3, which is mainly based on the

U-network architecture with specific modifications made for our custom design goal. The U-network architecture was first seen in U-net for medical image segmentation, and later proved to be good at image prediction where input and output pairs are spatially correlated. Specifically, the U-network is known to extract high-level spatial information from input feature maps (N × N × 2) through downsampling paths. In this case, strided convolution layers with generic hyperparameters (Height × Width × Channel) increase the effective receptive field, while the pooling layers help to make the network trainable and also aggregate information over large areas of the input feature maps, which can intuitively serve to reveal the relationship between the scatterer configuration and excitation field. However, in order to get paramount coarse features from the input image, downsampling shrinks the height and width of input images while enlarging the number of output channels to extract high-level features. Hence, an upsampling path is introduced to recover the original size of input images for per-pixel predictions [40], where transport convolution layers are used to collect coarse features from different channels to generate fine field predictions.

For our problem, the input feature maps consist of two stacked images with the size of N × N × 2 (N = 128), which refer to a scatterer's geometry and material composition, as well as the direction of the incident wave, respectively. The images, which exhibit the information of the incident plane waves, are binary ones as illustrated in Fig. 7 (c). The value "1" in these images denotes that the phase of the plane wave at this point is within in the range of [0, π), while "0" denotes the ranges of [$-\pi$, 0). Note that the phase of the plane wave at the center of the physical region is set to be zero to eliminate the multiplicity of solutions. Meanwhile, the propagation direction can also be obtained uniquely as below. At the center of the physical region, the direction which is perpendicular to the equiphasic surface and pointing from "1" to "0" is the propagation direction. The output contains the real and imaginary parts of the predicted EM fields with the same N × N × 2 (N = 128) size.

Next, faced with the large number of variations of the chosen scattering problem, a number of modifications were made: 1) short cut connection: the drawback of downsampling is the information loss. Hence, we implement upsampling with added short cut connections, which recovers the information from corresponding lower layers in the downsampling. This structure could improve the prediction accuracy. 2) Residual structure: multi-variant learning requires a large framework capacity, which can be expanded by adding more neural network layers, but accompanying problems such as degradation and vanishing gradients hinder the range of application. Employing a residual structure [41] with a gated structure [42] (see Fig. 4) guarantees optimization accuracy and fast convergence even when a considerable number of layers are utilized. Therefore, we integrate residual structure into every convolution/transport convolution operation and construct over 80 layers for EM field prediction. 3) Tailored designs of input and ouput channel: the proposed

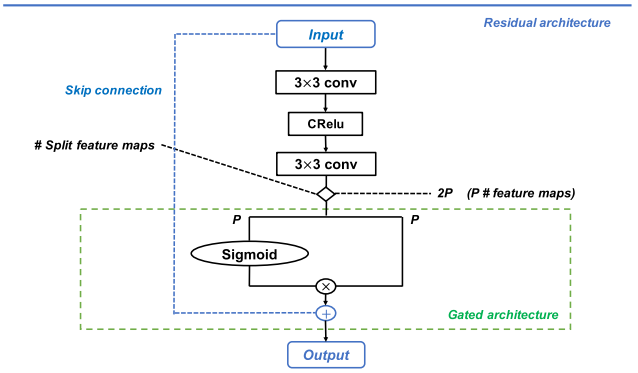

FIGURE 4. Schematic of the residual structure in the downsampling path.

framework incorporates the calculation of complex values, while generic image processing tasks via deep learning techniques are mostly conducted in the field of real numbers. Thus, it is of high necessity to make certain that the input and output schemes employed in the DL-framework can generated magnetic field distributions with complex-values. Towards this end, we separated real part and imaginary part of the complex value into different channels of deep neural network' input and output scheme (see Fig.3.), by which means the DL framework is able to calculate them parallelly.

As is illustrated in Fig. 3, the exact architectures are consistent during the respective downsampling and upsampling. There are six units, each of them consists of 2 residual blocks that implement downsampling step by step, in which one block contains 3 × 3 convolutional layers with a stride of 2, and the other one contains a 3 × 3 convolutional layer with a stride of 1. At every downsampling, the output channels double, while the input size reduces by a factor of 4. Additionally, 6 units with each consisting of 1 residual block and a 3 × 3 transport convolution layer implement upsampling step by step. At every upsampling, the output channels reduce by half, while input size scales up by a factor of 4. At the bottom of the U-shape architecture, one additional residual block containing a 3 × 3 convolutional layer with a stride of 1 is used to connect the downsampling and upsampling modules and essentially serves as an intermediate unit. Notably, each convolution / transport convolution layer is followed by CRelu to add nonlinearity. Moreover, we conduct sensitivity analysis to verify the effectiveness of increasing approximated accuracy via increasing the downsampling unit, the result is shown in Fig. 6b. It has been proven that more downsampling units could contribute to a larger network capacity, which is essential for better approximation of the proposed method. That being said, for our problem, 6 downsampling units are robust to generate satisfying optimization results.

Notably, it is an iterative process to adjust the aforementioned hyperparameters of our model in order to train the network properly, such as steps of the downsampling, the number of layers, the number of kernels, etc. Towards this end, we conduct the fine-tuning by referring

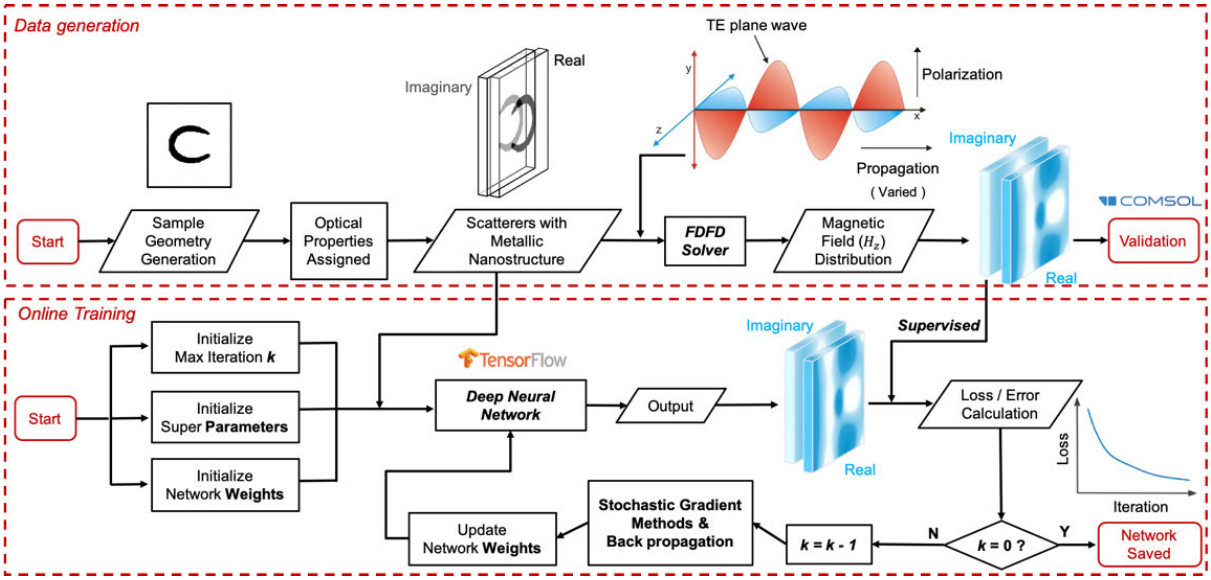

FIGURE 5. Algorithm block for data generation and DL framework training.

two main objectives. Firstly, the minimization of the error rate on the target test cases, which is important to denote the effectiveness of network-learning, such as generalized ability. Secondly, the feasibility of network-training, considering the memory and computational demand for the resource-limited training scenario. It is worth mentioning that we conduct several pre-experiments on the validation datasets based on the aforementioned principles and training skills of the neural network, in order to find the best set of hyperparameters which could maximize the performance of neural network. Holdout cross validation method is used for the 36000 set of datasets to test the viability of a set of hyperparameters' settings. After that, we applied the well-tuned neural network to the test dataset for the evaluation of performance, which we will further discuss in the Section III. and the final outcome proves the effectiveness of the chosen hyperparameters.

D. DL FRAMEWORK TRAINING

The proposed DL framework is implemented by using TensorFlow [43]. Moreover, an adaptive moment optimizer (Adam) [44] with a batch size of 16 is employed to optimize our pixel-wise loss function, which is given as follow:

$$Loss = \frac{1}{2}\sum_{i=1}^{N}\sum_{j=1}^{N}\left(F_{FDFD}\left(i,j\right) - F_{Framework}\left(i,j\right)\right)^2 \quad (18)$$

where F_{FDFD} (i, j) denotes the EM fields generated by the FDFD solver (ground truth) and $F_{Framework}$ (i, j) denotes the EM fields predicted by the proposed DL framework. Compared to a stochastic gradient (SGD) optimizer, Adam can converge faster for the chosen problem. The training process is started with a learning rate $\alpha = 2 \times 10^{-4}$ and a multiple decay rate $\beta = 0.96$ for every 5K iterations. In this case, exploding gradients are avoided which enables the network to achieve more precise convergence. The training was conducted on two NVIDIA GTX 1080 GPUs and took around 500K iterations and 15 h to reach convergence.

Figure 5 provides the detailed procedure for data generation and framework training. Figure 6 shows the learning curve of the proposed DL framework. While the training proceeds, the error rate decreases to an accepted level and once the value of loss remains stable in a small range the DL framework is considered successfully trained.

III. NUMERICAL RESULTS

Next, randomly chosen scatterer configurations from the test datasets are fed into the trained framework for magnetic field predictions along the z-direction. The numerical results generated from the randomly chosen set serve as a reference to evaluate the proposed DL framework from the perspectives of computational acceleration, accuracy and generalizability.

A. COMPUTATIONAL ACCELERATION

The main motivation behind using the proposed DL framework is that is enables faster predictions of the EM fields for random scatter configurations than traditional full-wave solvers. To this end, the DL framework utilizes the parallel computing ability of GPUs, which makes it possible to simultaneously predict large batches of inputs. As a result, 100 testing samples take only 1.76 s to generate their corresponding EM field distributions, which is three orders of magnitude faster than the 3626.2 s required by the FDFD solver.

B. ACCURACY

The proposed framework exhibits an excellent acceleration rate with uncompromising accuracy. The average relative error is used to evaluate the DL predictions. For a subdomain,

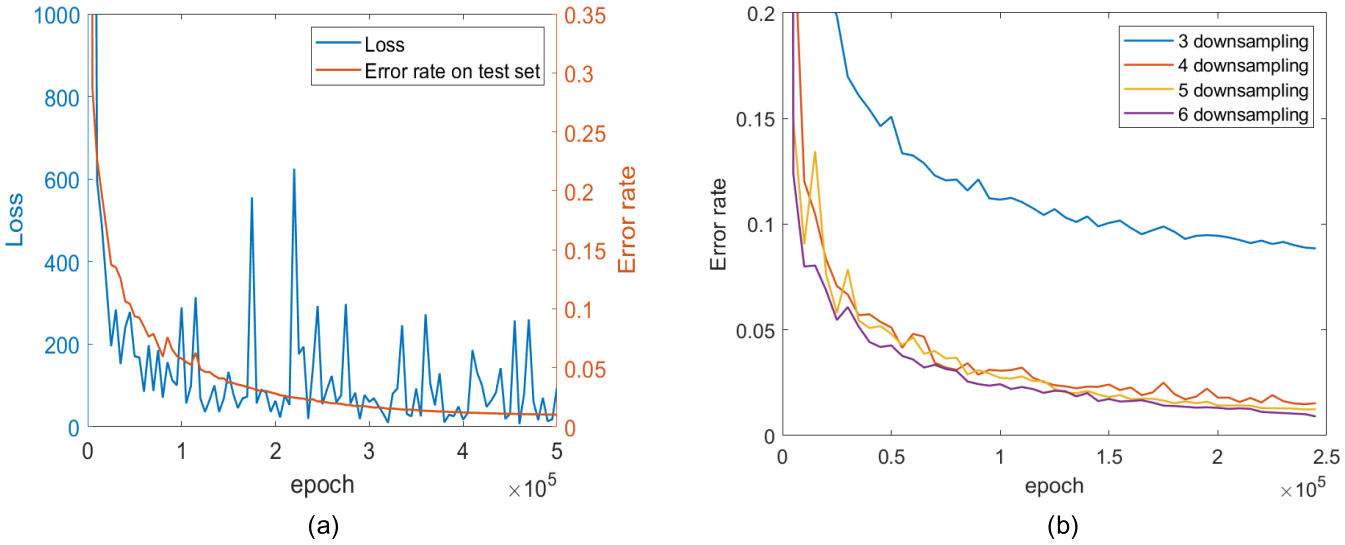

FIGURE 6. (a) Error rate and loss curve while training epochs proceed. (b) Error rate under different amounts of downsampling units while training epochs proceed.

the error function is formulated as follows:

$$Err\,(i,j) = \frac{\sqrt{\left(H_r\,(i,j) - H_r^{'}\,(i,j)\right)^2 + \left(H_i\,(i,j) - H_i^{'}\,(i,j)\right)^2}}{\sqrt{H_r^2\,(i,j) + H_i^2\,(i,j)}} \tag{19}$$

where H_r, H_i are the real and imaginary parts calculated by the FDFD solver, and $H_r^{'}, H_i^{'}$' are the real and imaginary parts predicted by the DL framework. The average relative error corresponds to the mean value over all 128×128 subdomains:

$$Err_{aver} = \frac{\sum_{i=1}^{128}\sum_{j=1}^{128} Err\,(i,j)}{128^2} \tag{20}$$

Figure 7 provides a clear view of the numerical results for randomly-selected test cases. Table 2 shows the average relative error rate in different testing categories, which generally lie in the range of 0.4%-1.2% per pixel. In total, the error rate is 0.792% per pixel compared to the ground truth, indicating excellent prediction capability, while figure 8 illustrates the statistical analysis of the average relative error rate distribution for each geometric category of deep learning framework predictions, FDFD simulation results are used as standard reference. Table 3 further shows the average relative error rate in terms of material selections. For most testing cases, the framework demonstrates robust prediction results, but it is inevitable to run the risk that a small portion (less than 5%) of the results will have significant errors.

C. GENERALIZATION ABILITY

It is important to verify that the developed DL framework learns the underlying physics of the problem, rather than simply overfitting between the trained data samples. This criterion is referred to as generalization ability. A representative measure to verify the DL framework's generalization

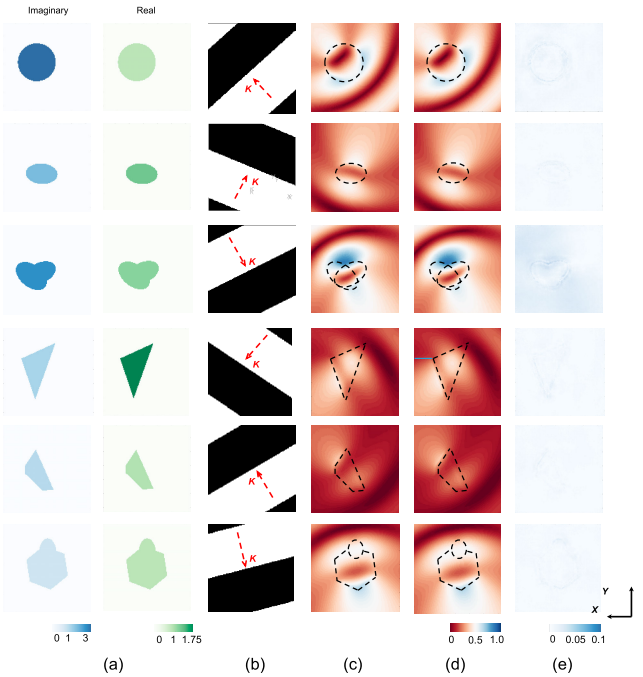

FIGURE 7. Numerical examples to demonstrate the performance of the network on test sets. (a) Geometric shape and permittivity of the scatterer, (b) Propagation direction of the incident wave, (c) Distribution of $|H_z|$ found via the FDFD method, (d) Distribution of $|H_z|$ predicted by the network, (e) Error distribution.

ability is to introduce open source datasets which have completely different nanostructure geometries than what exist in the training and test datasets. The open source dataset is expected to contain a large quantity of 2D objects with complicated geometric shapes. We further modified them by adding optical properties and fed them into the standard framework pipeline. Figure 9 summarizes the results of the open source test cases. Table 4 shows the average relative

TABLE 2. Average relative error rate for each geometric category of deep learning framework on the self-generated test dataset.

Categories	Size	Average Err
Circle	600	0.482%
Ellipse	600	0.539%
Hybrid	1200	1.124%
Pentagon	600	0.876%
Triangle	600	0.661%
Total	3600	0.792%

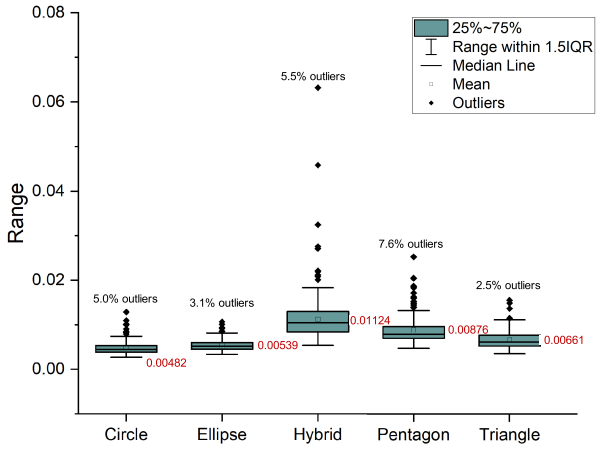

FIGURE 8. Statistical analysis of average relative error rate distribution of deep learning framework predictions on the self-generated test dataset.

TABLE 3. Average relative error rate for each material selection of deep learning framework predictions on the self-generated test dataset.

Categories	Average Err	Categories	Average Err
Cu	0.907%	Pt	1.127%
Ag	0.697%	Pd	0.604%
Au	0.786%	Hg	0.669%
Rh	0.620%	Ir	1.003%

error rate in these test cases, while Figure 10 shows the statistical analysis of the average relative error rate distribution for each geometric category of deep learning framework predictions, FDFD simulation results are used as standard reference. Table 5 further shows the average relative error rate in terms of material selections. For most testing cases, the framework demonstrates robust prediction results, but it is inevitable to run the risk that a small portion of the results will have significant errors. Also, to a minor extent, the framework suffers from accuracy degradation, which results from irregular geometric shape and low image resolution. Still, the average

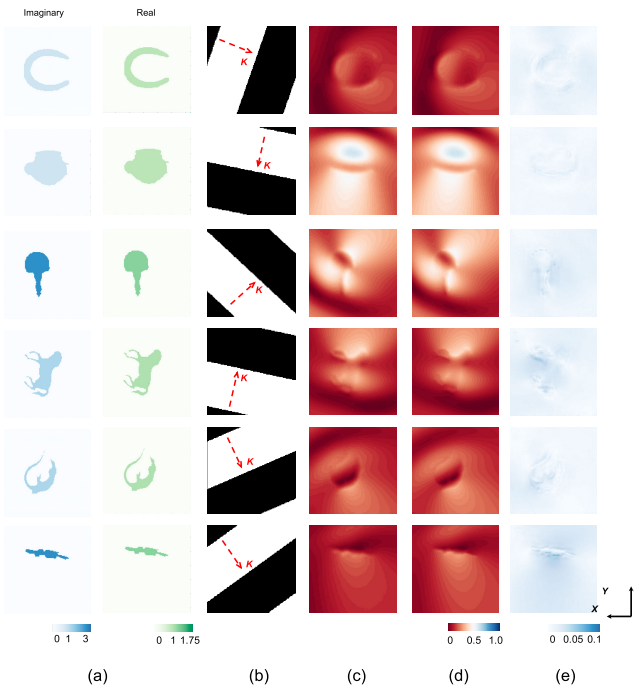

FIGURE 9. Numerical examples to demonstrate the performance of the network on an open-source dataset. (a) Geometric shape and permittivity of the scatterer, (b) Propagation direction of the incident wave, (c) Distribution of $|H_z|$ found via the FDFD method, (d) Distribution of $|H_z|$ predicted by the network, (e) Error distribution.

TABLE 4. Average relative error rate for each geometric category of deep learning framework predictions on the open-source dataset.

Categories	Size	Average Err
Open-source dataset	500	4.910%

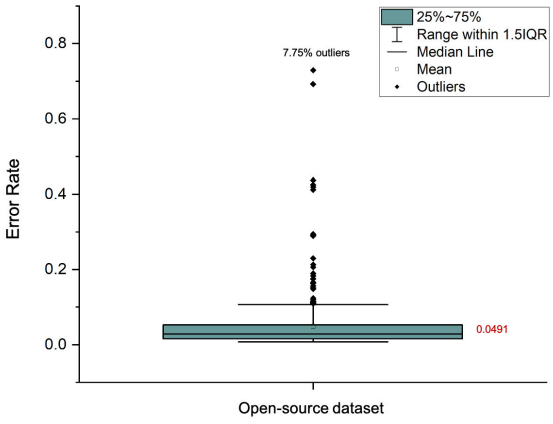

FIGURE 10. Statistical analysis of average relative error rate distribution of deep learning framework predictions on the open-source dataset.

relative error is robust at 4.910% per pixel compared with ground truth simulations, indicating a good generalization ability of the propose method, especially when the scatterer has subwavelength features.

TABLE 5. Average relative error rate for each material selection of deep learning framework predictions on the open-source dataset.

Categories	Average Err	Categories	Average Err
Cu	5.173%	Pt	9.163%
Ag	3.002%	Pd	3.749%
Au	4.478%	Hg	4.096%
Rh	2.893%	Ir	7.147%

IV. CONCLUSION AND PERSPECTIVE

In our study, we successfully constructed a DL framework to predict the magnetic field distribution of an isolated scatterer with complex nanostructure. We simulated the physical interaction between a pixel-based scatterer and an incident wave for a number of variations controlled by a set of trainable and controllable parameters. Our results confirm that the proposed DL framework is superior to a conventional FDFD solver which we used to generate a significant amount of training data in terms of high computational efficiency (three orders of magnitude acceleration) and low relative error rate (0.4%−1.2%). Moreover, open-source dataset-based testing verifies the generalizability of the proposed method. Consequently, with its robust generalizability and superior acceleration performance, our proposed method provides a guideline to develop faster 2D electrodynamic EM solvers for the simulation of a wide variety of nanophotonic devices, which can also be applied to scatterers with large field enhancement or with targeted bandwidths in future studies. With our proposed DL method, it is straightforward to analysis more complex nano-optical near-filed effects without specific modeling for different nanostructures. Besides, we anticipate the computational domain of our proposed DL-based solvers could be extended to 3D domain with similar working scheme. Toward this end, more efforts need to be done to construct 3D dataset, and redesign some parts of deep neural network's architecture.

Additionally, from the designer's point of view, inverse-problems which involve using simulated responses to predict nanostructure behaviors also face obstacles such as inefficiency and being ill-posed with high complexity. Notably, the proposed deep learning framework has the feature of symmetrical input and output format, as well as corresponding convolution and deconvolution units. It demonstrates great potential to solve inverse problems with the same training and testing procedure as the scattering problem. Last but not least, the as-developed method can accommodate more input parameters by simply stacking the input images, which means additional scattering conditions can be addressed for nano-structures targeted for other specific applications. We anticipate our proposed DL approach can be extensively adopted in a wide variety of scenarios in nanophotonics, providing an alternative for fast and universal electromagnetic simulations.

ACKNOWLEDGMENT

(Yongzhong Li and Yinpeng Wang contributed equally to this work.)

REFERENCES

[1] L. Zhou, Y. Tan, J. Wang, W. Xu, Y. Yuan, W. Cai, S. Zhu, and J. Zhu, "3D self-assembly of aluminium nanoparticles for plasmon-enhanced solar desalination," *Nature Photon.*, vol. 10, no. 6, pp. 393–398, Jun. 2016.

[2] A. Kinkhabwala, Z. Yu, S. Fan, Y. Avlasevich, K. Müllen, and W. E. Moerner, "Large single-molecule fluorescence enhancements produced by a bowtie nanoantenna," *Nature Photon.*, vol. 3, no. 11, pp. 654–657, Nov. 2009.

[3] M. Turkmen, S. Aksu, A. Çetin, A. A. Yanik, and H. Altug, "Multi-resonant metamaterials based on UT-shaped nano-aperture antennas," *Opt. Express*, vol. 19, no. 8, pp. 7921–7928, 2011.

[4] E. A. Semouchkina, G. B. Semouchkin, M. Lanagan, and C. A. Randall, "FDTD study of resonance processes in metamaterials," *IEEE Trans. Microw. Theory Techn.*, vol. 53, no. 4, pp. 1477–1487, Apr. 2005.

[5] S. D. Campbell, D. Sell, R. P. Jenkins, E. B. Whiting, J. A. Fan, and D. H. Werner, "Review of numerical optimization techniques for meta-device design," *Opt. Mater. Express*, vol. 9, no. 4, pp. 1842–1863, 2019.

[6] A. Taflove, A. Oskooi, and S. G. Johnson, *Advances in FDTD Computational Electrodynamics: Photonics and nanotechnology*. Norwood, MA, USA: Artech House, 2013.

[7] M. Kim, W. Choi, Y. Choi, C. Yoon, and W. Choi, "Transmission matrix of a scattering medium and its applications in biophotonics," *Opt. Express*, vol. 23, no. 10, pp. 12648–12668, 2015.

[8] J.-M. Jin, *The Finite Element Method in Electromagnetics*. Hoboken, NJ, USA: Wiley, 2015.

[9] R. F. Harrington, *Field Computation by Moment Methods*. Hoboken, NJ, USA: Wiley, 1993.

[10] A. Taflove and S. C. Hagness, *Computational Electrodynamics: The Finite-difference Time-domain Method*. Norwood, MA, USA: Artech House, 2005.

[11] J. Chen and Q. H. Liu, "Discontinuous Galerkin time-domain methods for multiscale electromagnetic simulations: A review," *Proc. IEEE*, vol. 101, no. 2, pp. 242–254, Feb. 2013.

[12] Q. Zhan, Q. Sun, Q. Ren, Y. Fang, H. Wang, and Q. H. Liu, "A discontinuous Galerkin method for simulating the effects of arbitrary discrete fractures on elastic wave propagation," *Geophys. J. Int.*, vol. 210, no. 2, pp. 1219–1230, Aug. 2017.

[13] P. Wen, Q. Ren, J. Chen, A. Chen, and Y. Zhang, "Improved memory efficient subdomain level discontinuous Galerkin time domain method for Periodic/Quasi-periodic structures," *IEEE Trans. Antennas Propag.*, early access, Jun. 3, 2020, doi: 10.1109/TAP.2020.2998215.

[14] J. Smajic, C. Hafner, L. Raguin, K. Tavzarashvili, and M. Mishrikey, "Comparison of numerical methods for the analysis of plasmonic structures," *J. Comput. Theor. Nanoscience*, vol. 6, no. 3, pp. 763–774, Mar. 2009.

[15] N. Liu, M. Hentschel, T. Weiss, A. P. Alivisatos, and H. Giessen, "Three-dimensional plasmon rulers," *Science*, vol. 332, no. 6036, pp. 1407–1410, Jun. 2011.

[16] C. Sönnichsen, B. M. Reinhard, J. Liphardt, and A. P. Alivisatos, "A molecular ruler based on plasmon coupling of single gold and silver nanoparticles," *Nature Biotechnol.*, vol. 23, no. 6, pp. 741–745, Jun. 2005.

[17] K. Yao, R. Unni, and Y. Zheng, "Intelligent nanophotonics: Merging photonics and artificial intelligence at the nanoscale," *Nanophotonics*, vol. 8, no. 3, pp. 339–366, Jan. 2019.

[18] A. Y. Piggott, J. Lu, K. G. Lagoudakis, J. Petykiewicz, and T. M. Babinec, "Inverse design and demonstration of a compact and broadband on-chip wavelength demultiplexer," *Nature Photon.*, vol. 9, no. 6, pp. 374–377, Jun. 2015.

[19] Y. Li, Y. Xu, M. Jiang, B. Li, T. Han, C. Chi, F. Lin, B. Shen, X. Zhu, L. Lai, and Z. Fang, "Self-learning perfect optical chirality via a deep neural network," *Phys. Rev. Lett.*, vol. 123, no. 21, Nov. 2019, Art. no. 213902.

[20] I. Goodfellow, Y. Bengio, and A. Courville, *Deep Learning*. Cambridge, MA, USA: MIT Press, 2016.

[21] A. Massa, D. Marcantonio, X. Chen, M. Li, and M. Salucci, "DNNs as applied to electromagnetics, antennas, and Propagation—A review," *IEEE Antennas Wireless Propag. Lett.*, vol. 18, no. 11, pp. 2225–2229, Nov. 2019.

[22] A. Dosovitskiy, P. Fischer, E. Ilg, P. Hausser, C. Hazirbas, V. Golkov, P. V. D. Smagt, D. Cremers, and T. Brox, "FlowNet: Learning optical flow with convolutional networks," in *Proc. IEEE Int. Conf. Comput. Vis. (ICCV)*, Dec. 2015, pp. 2758–2766.
[23] X. Guo, W. Li, and F. Iorio, "Convolutional neural networks for steady flow approximation," in *Proc. 22nd ACM SIGKDD Int. Conf. Knowl. Discovery Data Mining*, Aug. 2016, pp. 481–490.
[24] J. Peurifoy, Y. Shen, L. Jing, Y. Yang, F. Cano-Renteria, B. G. DeLacy, J. D. Joannopoulos, and M. Tegmark, "Nanophotonic particle simulation and inverse design using artificial neural networks," *Sci. Adv.*, vol. 4, no. 6, Jun. 2018, Art. no. eaar4206.
[25] W. Tang, T. Shan, X. Dang, M. Li, F. Yang, S. Xu, and J. Wu, "Study on a Poisson's equation solver based on deep learning technique," in *Proc. IEEE Electr. Design Adv. Packag. Syst. Symp. (EDAPS)*, Dec. 2017, pp. 1–3.
[26] T. Shan, X. Dang, M. Li, F. Yang, S. Xu, and J. Wu, "Study on a 3D Possion's equation slover based on deep learning technique," in *Proc. IEEE Int. Conf. Comput. Electromagn. (ICCEM)*, Mar. 2018, pp. 1–3.
[27] H. M. Yao and L. J. Jiang, "Machine learning based neural network solving methods for the FDTD method," in *Proc. IEEE Int. Symp. Antennas Propag. USNC/URSI Nat. Radio Sci. Meeting*, Jul. 2018, pp. 2321–2322.
[28] A. Khan, V. Ghorbanian, and D. Lowther, "Deep learning for magnetic field estimation," *IEEE Trans. Magn.*, vol. 55, no. 6, Jun. 2019, Art. no. 7202304.
[29] I. Sajedian, J. Kim, and J. Rho, "Finding the optical properties of plasmonic structures by image processing using a combination of convolutional neural networks and recurrent neural networks," *Microsyst. Nanoengineering,* vol. 5, no. 1, pp. 1–8, Dec. 2019.
[30] Y. Kiarashinejad, S. Abdollahramezani, M. Zandehshahvar, O. Hemmatyar, and A. Adibi, "Deep learning reveals underlying physics of Light–Matter interactions in nanophotonic devices," *Adv. Theory Simul.*, vol. 2, no. 9, Sep. 2019, Art. no. 1900088.
[31] Y. Kiarashinejad, M. Zandehshahvar, S. Abdollahramezani, O. Hemmatyar, R. Pourabolghasem, and A. Adibi, "Knowledge discovery in nanophotonics using geometric deep learning," *Adv. Intell. Syst.*, vol. 2, no. 2, Feb. 2020, Art. no. 1900132.
[32] Y. Kiarashinejad, S. Abdollahramezani, and A. Adibi, "Deep learning approach based on dimensionality reduction for designing electromagnetic nanostructures," *npj Comput. Mater.*, vol. 6, no. 1, pp. 1–12, Dec. 2020.
[33] P. R. Wiecha and O. L. Muskens, "Deep learning meets nanophotonics: A generalized accurate predictor for near fields and far fields of arbitrary 3D nanostructures," *Nano Lett.*, vol. 20, no. 1, pp. 329–338, Jan. 2020.
[34] O. Ronneberger, P. Fischer, and T. Brox, "U-net: Convolutional networks for biomedical image segmentation," in *Proc. Int. Conf. Med. Image Comput. Comput.-Assist. Intervent.*, 2015, pp. 234–241.
[35] W. B. Zimmerman, *Multiphysics Modeling with Finite Element Methods*. Singapore: World Scientific, 2006.
[36] D. R. Lide, *CRC Handbook of Chemistry and Physics*. Boca Raton, FL, USA: CRC Press, 2004.
[37] V. Simoncini and D. B. Szyld, "Recent computational developments in Krylov subspace methods for linear systems," *Numer. Linear Algebra Appl.*, vol. 14, no. 1, pp. 1–59, 2007.
[38] M. R. Hestenes and E. Stiefel, *Methods of Conjugate Gradients for Solving Linear Systems*. Washington, DC, USA: NBS, 1952.
[39] A. Carlier, K. Leonard, S. Hahmann, G. Morin, and M. Collins, "The 2D shape structure dataset: A user annotated open access database," *Comput. Graph.*, vol. 58, pp. 23–30, Aug. 2016.
[40] T. Salimans, A. Karpathy, X. Chen, and D. P. Kingma, "PixelCNN++: Improving the PixelCNN with discretized logistic mixture likelihood and other modifications," 2017, *arXiv:1701.05517*. [Online]. Available: http://arxiv.org/abs/1701.05517
[41] K. He, X. Zhang, S. Ren, and J. Sun, "Deep residual learning for image recognition," in *Proc. IEEE Conf. Comput. Vis. Pattern Recognit. (CVPR)*, Jun. 2016, pp. 770–778.
[42] H. Wang, Y. Wang, Q. Zhang, S. Xiang, and C. Pan, "Gated convolutional neural network for semantic segmentation in high-resolution images," *Remote Sens.*, vol. 9, no. 5, p. 446, May 2017.
[43] M. Abadi, "Tensorflow: A system for large-scale machine learning," in *Proc. 12th Symp. Oper. Syst. Des. Implement. (OSDI)*, 2016, pp. 265–283.
[44] D. P. Kingma and J. Ba, "Adam: A method for stochastic optimization," 2014, *arXiv:1412.6980*. [Online]. Available: http://arxiv.org/abs/1412.6980

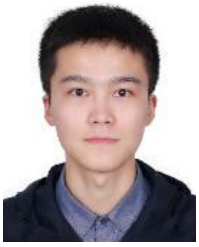

YONGZHONG LI received the B.S. degree (Hons.) in electronic and information engineering from Beihang University, Beijing, China, in 2020. He will pursue the Ph.D. degree in electrical and computer engineering with The University of Texas at Austin. His current research interests include multi-physics modeling, deep learning, and flexible electronics in terms of nanomaterials and nanophotonics. He received the Best Undergraduate Thesis Award.

YINPENG WANG received the B.S. degree in electronic and information engineering from Beihang University, in 2020, where he is currently pursuing the M.S. degree in electronic and information engineering. From 2017 to 2018, he was a Researcher at the Physical Experiment Center, Beihang University. In 2018, he worked as a Research Assistant with the Spintronics Interdisciplinary Center. Since 2019, he has been a member of the Institute of EMC Technology, under the supervision of Prof. Q. Ren. His current research interests include electromagnetic scattering, inverse scattering, deep learning, and computational multi-physical fields. He serves as a Reviewer for IOP journals.

SHUTONG QI received the B.S. degree (Hons.) in electrical engineering from Beihang University, Beijing, China, in 2020. He is currently pursuing the Ph.D. degree with the Electrical and Computer Engineering Department, University of Toronto. From 2018 to 2020, he was a Research Assistant at the Institute of EMC Technology, under the supervision of Prof. Q. Ren. In Summer 2019, he worked as an Intern at the XDiscovery Lab, Dartmouth College. His current research interests include numerical electromagnetic method, machine learning and computational multi-physical fields, and human–computer interaction.

QIANG REN (Member, IEEE) received the B.S. degree in electrical engineering from Beihang University, Beijing, China, in 2008, and the M.S. degrees in electrical engineering from the Institute of Acoustics, Chinese Academy of Sciences, Beijing, in 2011, and the Ph.D. degree in electrical engineering from Duke University, Durham, NC, USA, in 2015. From 2016 to 2017, he was a Postdoctoral Researcher with the Computational Electromagnetics and Antennas Research Laboratory (CEARL), The Pennsylvania State University, University Park, PA, USA. In September 2017, he joined the School of Electronics and Information Engineering, Beihang University, Beijing, China, as an "Excellent Hundred" Associate Professor. His current research interests include numerical methods for multiscale and multiphysics modeling, metasurfaces, inverse scattering, and parallel computing. He was a recipient of the Young Scientist Award of 2018 International Applied Computational Electromagnetics Society (ACES) Symposium in China. He serves as an Associate Editor of *ACES Journal* and *Microwave and Optical Technology Letters* (MOTL), and also serves as a reviewer for 30 journals.

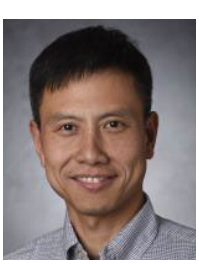

LEI KANG received the B.S. degree in applied physics and the M.S. degree in optical engineering from Northwestern Polytechnical University, Xi'an, China, in 2002 and 2005, respectively, and the Ph.D. degree in material science and engineering from Tsinghua University, Beijing, China, in 2010. He was a Postdoctoral Researcher at IEMN, Université des Sciences et Technologies de Lille, Villeneuve-d'Ascq, France, from 2010 to 2011, at the Liquid Crystal Institute, Kent State University, Kent, OH, USA, from 2011 to 2012, and at LAPO, Georgia

Institute of Technology, Atlanta, GA, USA, from 2012 to 2014. He is currently an Assistant Research Professor with the Department of Electrical Engineering, The Pennsylvania State University, University Park, PA, USA. His current research interests include metamaterials at both RF and optical frequencies, and nanophotonics.

SAWYER D. CAMPBELL (Member, IEEE) received the B.S. degree in physics from Illinois Wesleyan University, Bloomington, IL, USA, in 2008, and the M.S. and Ph.D. degrees in optical sciences from The University of Arizona, Tucson, AZ, USA, in 2010 and 2013, respectively. He was an Undergraduate Researcher with the Department of Physics, Intense Laser Physics Theory Unit, Illinois State University, from 2004 to 2008. He was also a Graduate Research Associate with the "La Casa de Creative Electromagneticists" group, Department of Electrical and Computer Engineering, The University of Arizona, under the advisement of Prof. Richard W. Ziolkowski. In 2014, he joined the Computational Electromagnetics and Antennas Research Laboratory, Department of Electrical Engineering, The Pennsylvania State University, as a Postdoctoral Scholar, under the supervision of Prof. D. H. Werner, where he has been with the Department of Electrical Engineering, since 2018, as an Assistant Research Professor. He has extensive experience in the computational modeling and inverse design of metamaterial- and transformation optics-based devices at RF, infrared, and optical frequencies. He is an expert in the application of multi-objective and surrogate-assisted optimization techniques to challenging problems in both the RF and optical regimes. He has published over 80 technical articles and proceedings articles and is the author/coauthor of three book chapters. His current research interests include light scattering, plasmonics, transformation optics, geometrical optics, gradient-index lens design, topological- and surrogate model-assisted optimization and inverse-design of nanoantenna- and metasurface-based devices, and the applications of deep learning to RF and optical inverse-design problems. He is a member of APS, OSA, and SPIE, and is the past Chair and Current Vice-Chair/Treasurer of the IEEE Central Pennsylvania Section.

PINGJUAN L. WERNER (Senior Member, IEEE) is currently a Professor with the College of Engineering, The Pennsylvania State University, where she is also a Fellow of the Leonhard Center, College of Engineering. Her primary research focuses in the area of electromagnetics, including fractal antenna engineering and the application of genetic algorithms in electromagnetics. She is a member of Tau Beta Pi National Engineering Honor Society, Eta Kappa Nu National Electrical Engineering Honor Society, and Sigma Xi National Research Honor Society. She received the Best Paper Award from the Applied Computational Electromagnetics Society, in 1993.

DOUGLAS H. WERNER (Fellow, IEEE) received the B.S., M.S., and Ph.D. degrees in electrical engineering and the M.A. degree in mathematics from The Pennsylvania State University (Penn State), University Park, in 1983, 1985, 1989, and 1986, respectively.

He holds the John L. and Genevieve H. McCain Chair Professorship at the Department of Electrical Engineering, The Pennsylvania State University. He is the Director of the Computational Electromagnetics and Antennas Research Lab and a member of the Communications and Space Sciences Lab (CSSL). He is also a Faculty Member of the Materials Research Institute (MRI), Penn State. He has published over 900 technical papers and proceedings articles, is the author of 30 book chapters with several additional chapters currently in preparation, and holds 20 patents. He has published several books, including *Frontiers in Electromagnetics* (IEEE Press, 2000), *Genetic Algorithms in Electromagnetics* (Wiley/IEEE, 2007), *Transformation Electromagnetics and Metamaterials: Fundamental Principles and Applications* (Springer, 2014), *Electromagnetics of Body Area Networks: Antennas, Propagation, and RF Systems* (Wiley/IEEE, 2016), and *Broadband Metamaterials in Electromagnetics: Technology and Applications* (Pan Stanford Publishing, 2017). He has also contributed chapters for several books, including *Electromagnetic Optimization by Genetic Algorithms* (Wiley Interscience, 1999), *Soft Computing in Communications* (Springer, 2004), *Antenna Engineering Handbook* (McGraw-Hill, 2007), *Frontiers in Antennas: Next Generation Design and Engineering* (McGraw-Hill, 2011), *Numerical Methods for Metamaterial Design* (Springer, 2013), *Computational Electromagnetics* (Springer, 2014), *Graphene Science Handbook: Nanostructure and Atomic Arrangement* (CRC Press, 2016), the *Handbook of Antenna Technologies* (Springer, 2016), and *Transformation Wave Physics: Electromagnetics, Electrodynamics and Thermodynamics* (CRC Press, 2016). His research interests include computational electromagnetics (MoM, FEM, FEBI, FDTD, DGTD, CBFM, RCWA, GO, and GTD/UTD) antenna theory and design, phased arrays (including ultra-wideband arrays), microwave devices, wireless and personal communication systems (including on-body networks), wearable and e-textile antennas, RFID tag antennas, conformal antennas, reconfigurable antennas, frequency selective surfaces, electromagnetic wave interactions with complex media, metamaterials, electromagnetic bandgap materials, zero and negative index materials, transformation optics, nanoscale electromagnetics (including nanoantennas), fractal and knot electrodynamics, and nature-inspired optimization techniques (genetic algorithms, clonal selection algorithms, particle swarm, wind driven optimization, and various other evolutionary programming schemes). He is a Fellow of the IET, OSA, ACES, and PIERS EMA. He is a member of URSI Commissions B and G, Eta Kappa Nu, Tau Beta Pi, and Sigma Xi. He is also a Senior Member of the National Academy of Inventors (NAI), the International Union of Radio Science (URSI), and the Society of Photo-Optical Instrumentation Engineers (SPIE). He received the 1993 Applied Computational Electromagnetics Society (ACES) Best Paper Award and was also a recipient of the 1993 International Union of Radio Science (URSI) Young Scientist Award. In 1994, he received the Pennsylvania State University Applied Research Laboratory Outstanding Publication Award. He was a coauthor (with one of his graduate students) of an article published in the IEEE TRANSACTIONS ON ANTENNAS AND PROPAGATION, which received the 2006 R. W. P. King Award. He received the inaugural IEEE Antennas and Propagation Society Edward E. Altshuler Prize Paper Award and the Harold A. Wheeler Applications Prize Paper Award, in 2011 and 2014, respectively. He also received the DoD Ordnance Technology Consortium (DOTC) Outstanding Technical Achievement Award, in 2018, the 2015 ACES Technical Achievement Award, the 2019 ACES Computational Electromagnetics Award, and the IEEE Antennas and Propagation Society 2019 Chen-To Tai Distinguished Educator Award. He was a recipient of the College of Engineering PSES Outstanding Research Award and the Outstanding Teaching Award, in March 2000 and March 2002, respectively. He was also presented with the IEEE Central Pennsylvania Section Millennium Medal. In March 2009, he received the PSES Premier Research Award. he is a former Associate Editor of *Radio Science*, a former Editor of the *IEEE Antennas and Propagation Magazine*, an Editorial Board Member of *Scientific Reports* (a Nature sub-journal), an Editorial Board Member of *EPJ Applied Metamaterials*, and an Editor of the IEEE Press Series on Electromagnetic Wave Theory & Applications.